



HAL
open science

Impedimetric sensors based on diethylphosphonate-containing poly(arylene ether nitrile)s films for the detection of lead ions

Taha Chabbah, Saber Chatti, Nicole Jaffrezic-Renault, Steffen Weidner, C. Marestin, Régis Mercier

► To cite this version:

Taha Chabbah, Saber Chatti, Nicole Jaffrezic-Renault, Steffen Weidner, C. Marestin, et al.. Impedimetric sensors based on diethylphosphonate-containing poly(arylene ether nitrile)s films for the detection of lead ions. *Polymers for Advanced Technologies*, 2023, 34 (8), pp.2471-2481. 10.1002/pat.6065 . hal-04540521

HAL Id: hal-04540521

<https://hal.science/hal-04540521>

Submitted on 10 Apr 2024

HAL is a multi-disciplinary open access archive for the deposit and dissemination of scientific research documents, whether they are published or not. The documents may come from teaching and research institutions in France or abroad, or from public or private research centers.

L'archive ouverte pluridisciplinaire **HAL**, est destinée au dépôt et à la diffusion de documents scientifiques de niveau recherche, publiés ou non, émanant des établissements d'enseignement et de recherche français ou étrangers, des laboratoires publics ou privés.

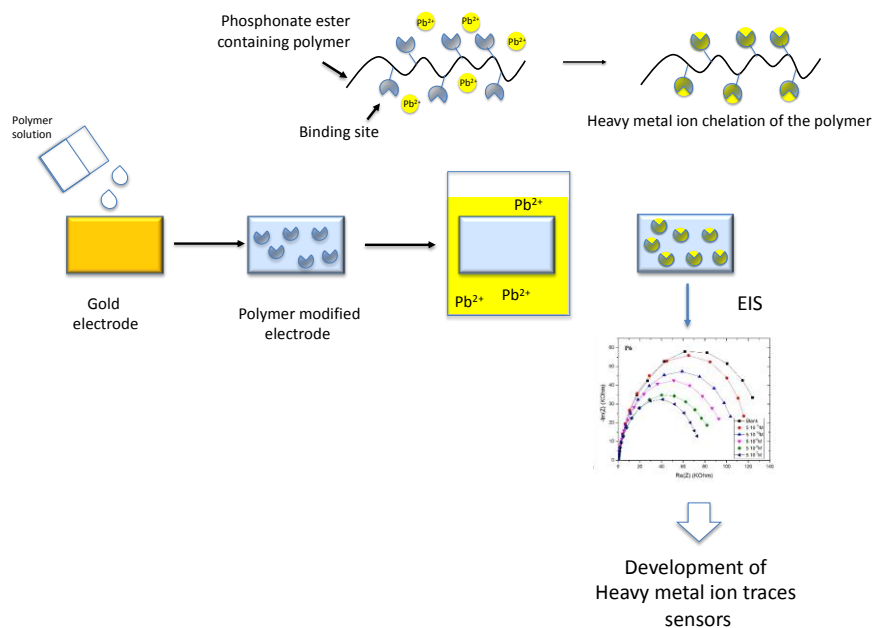
Impedimetric sensors based on diethylphosphonate-containing poly(arylene ether nitrile)s films for the detection of lead ions

Taha Chabbah⁽¹⁾, Saber Chatti⁽¹⁾, Nicole Jaffrezic-Renault⁽²⁾, Steffen Weidner⁽³⁾

Catherine Marestin⁽⁴⁾, Regis Mercier⁽⁴⁾

- ⁽¹⁾ National Institute of Research and Physico-chemical Analysis (INRAP), Biotechnopole of Sidi Thabet, 2020 Ariana, Tunisia
- ⁽²⁾ University of Lyon, Institute of Analytical Sciences (ISA), UMR 5280, 69100 Villeurbanne, France
- ⁽³⁾ Bundesanstalt für Materialforschung und prüfung (BAM) Fachbereich 6.3 “Strukturanalytik” Richard-Willstätter-Strasse 11, 12489 Berlin Germany
- ⁽⁴⁾ University of Lyon, INSA-Lyon, CNRS, IMP UMR 5223, F-69 621 Villeurbanne Cedex, France

Table of content



Impedimetric sensors based on diethylphosphonate-containing poly(arylene ether nitrile)s films for the detection of lead ions

Taha Chabbah⁽¹⁾, Saber Chatti⁽¹⁾, Nicole Jaffrezic-Renault^{*(2)}, Steffen Weidner⁽³⁾
Catherine Marestin⁽⁴⁾, Regis Mercier⁽⁴⁾

⁽¹⁾ National Institute of Research and Physico-chemical Analysis (INRAP), Biotechnopole of Sidi Thabet, 2020 Ariana, Tunisia

⁽²⁾ University of Lyon, Institute of Analytical Sciences (ISA), UMR 5280, 5 Rue de la Doua, 69100 Villeurbanne, France

⁽³⁾ Bundesanstalt für Materialforschung und prüfung (BAM) Fachbereich 6.3 “Strukturanalytik” Richard-Willstätter-Strasse 11, 12489 Berlin Germany

⁽⁴⁾ University of Lyon, INSA-Lyon, CNRS, IMP UMR 5223, F-69 621 Villeurbanne Cedex, France

*Corresponding author’s e-mail address: nicole.jaffrezic@univ-lyon1.fr

Abstract

This article describes the elaboration and characterization of diethylphosphonate-containing polymers coated electrodes as sensors for the detection of heavy metals traces, by Electrochemical Impedance Spectroscopy.

Diethylphosphonate groups were chosen as heavy metals binding sites. Two different series of polymers bearing these anchoring groups were synthesized. Whereas the diethylphosphonate groups are directly incorporated in the aromatic macromolecular chain in some polymers, an aliphatic spacer is removing the chelating site from the polymer backbone in others. The influence of the macromolecular structure on the sensing response was studied, especially for the detection of Pb^{2+} , Ni^{2+} , Cd^{2+} and Hg^{2+} . Polymer P6, including the higher amount of diethylphosphonate groups removed from the polymer chain by a short alkyl spacer gave the higher sensitivity of detection of lead ions, with a detection limit of 50 pM.

Keywords

Phosphonate ester-containing poly(arylene ether nitrile)s; alkyl spacer; heavy metal detection; lead ions.

1. Introduction

Because of their high toxicity and bio-accumulative potential, heavy metals (and especially lead) are considered as very harmful pollutants. Indeed, it is well-established that even traces levels of such compounds can induce irreversible and deleterious effects to many vital human organs. Due to the ever-growing pollution caused by domestic, agricultural or industrial wastes, environmental issues have become a major concern. The accurate determination of heavy metal ions present in various effluents is therefore of utmost importance to assess their levels of contamination. As mentioned by the Water Framework Directive (WFD) [1] the Environmental Quality Standards (EQS) threshold values for Ni, Cd, Pb, and Hg should be respectively, 341, 0.7–2.2, 35, and 0.25 nM.

Conventional analytical detection methods such as atomic absorption spectroscopy (AAS) [2], inductively coupled plasma/atomic emission spectrometry (ICP-AES) [3] or inductively coupled plasma/mass spectrometry (ICP-MS) [4] are very sensitive but rather complex to use because they require very expensive equipment as well as specific skills for reliable assessment. Thanks to their usual intrinsic characteristics (high sensitivity, short analytical time, low cost), electrochemical sensors appear as very promising tools for the detection of heavy metal ions [5]. However, the development of selective chemical sensors susceptible to detect traces levels of lead ions is still today a real challenge.

Ion-complexing polymers coated electrodes have attracted a specific interest in the last decade. The presence of oxygen, nitrogen or phosphorus atoms in the macromolecular structures were evidenced to favor the complexation of heavy metal ions. Phosphorus-containing materials have recently been the subject of more specifically extensive research, highlighting peculiar and interesting properties. Their complexing and chelating properties as well as their ability to bind metallic cations are outstanding. Such materials are therefore usually used as dispersant, corrosion inhibition agent or to prevent deposit formation [6]. Phosphorus atoms can be incorporated in polymers under different forms [7]. Phosphates (O-PO(OH)_2) [8], phosphoramides ($\text{RR}'\text{-(PO)-NR}'_2$) [9], phosphonates esters (R-PO(OR)_2) or phosphonic acids (R-PO(OH)_2) [10-14] have gained a special interest because of their fascinating properties and potential applications in many fields. Phosphonic acids are especially useful in ion-exchange materials, are incorporated in membranes (in paper and textile industry) for biomedical purposes, in desalination systems [15], in proton exchange membranes for fuel cell applications [16, 17] or are used to chelate rare earth elements [18]. However, the incorporation of high proportions of phosphonic acids in high performance

polymers for the elaboration of sensors is still problematic, because of the low solubility of the resulting structures.

In the frame of ongoing research work related to the development of new aromatic macromolecular structures, we recently published new insights for the synthesis of phosphonate ester containing poly(arylether)s [19]. Such polymers are readily soluble in common organic solvent, and can be casted into thin films, as required for the preparation of sensors. Our expertise in the synthesis of these polymers and recent interesting work concerning the chelation properties of phosphonate ester groups towards lanthanides [20], prompted us to evaluate their chelating properties towards heavy metal ions, and in particular lead ions.

This work reports the design, synthesis and characterization of functional polymers with phosphonate esters sites side-groups. Electrochemical Impedance Spectroscopy (EIS) measurements were performed using gold electrodes coated with these polymers, in the presence of heavy metal ions (lead, nickel, cadmium, mercury). An evidence of a correlation between logarithm of the lead and other ion concentrations present in the tested solution and the electrochemical impedance of the polymer-modified gold electrode/ electrolyte interface was clearly established. The obtained results suggest that such polymer-modified electrodes could be used as selective and sensitive sensors for the detection of traces levels of lead ions in aqueous media.

1.-Experimental Section

1.1. Materials

All chemicals were provided by Aldrich. 2,2-Bis(4-hydroxyphenyl)propane (Bisphenol A) was purified by crystallization. 5-chloropentanone was distilled prior to use. Dimethyl sulfoxide (DMSO), potassium carbonate and other chemicals (2,6-difluorobenzonitrile, phenol, NaI, triethyl phosphite, diethylphosphite, dibromofluorenone, trifluoromethane sulfonic acid, etc.) were used as received.

1.2. Characterization Methods

Nuclear Magnetic Resonance spectra (^1H , ^{13}C and ^{31}P) were recorded on a Bruker Avance 400 spectrometer (Brucker France, Wissembourg) (operation frequencies of 400.16 MHz for ^1H , 100.63 MHz for ^{13}C , and 161.99 MHz for ^{31}P). Tetramethylsilane was used as internal standard for ^1H and ^{13}C spectra.

An Autoflex Max MALDI mass spectrometer (Bruker Daltonik, Bremen, Germany) was used for mass spectrometric analysis. Spectra were recorded in the reflector instrument mode. The samples were dissolved in Dimethylformamide. DCTB (trans-2-[3-(4-tert-butylphenyl)-2-methyl-2-propenylidene] malononitrile, was used as a matrix and doped with KTFA (potassium trifluoroacetate) to selectively enable the formation of potassium adduct ions.

Dynamic Thermogravimetric analyses (TGA) were performed on a TA Q50 Instrument (TA Instruments France, Guyancourt), under air, at 10°C/min. The polymer glass transition temperatures (T_g) were determined by Differential Scanning Calorimetry (DSC) with a Mettler-Toledo DSC822e equipment (Mettler-Toledo SAS, Viroflay, France), at 10 °C/min and under nitrogen.

Electrochemical impedance spectroscopy measurements were carried out using a potentiostat (Biologic-EC-Lab VMP3) analyzer. A 5 cm³ Pyrex glass electrochemical cell equipped with the polymer-modified electrode acting as working electrode (0.07 cm² active area), an Ag/AgCl/ reference electrode, and a Platinum counter electrode was used. The polymer-modified gold electrode was equilibrated in aqueous solutions containing different metallic ions concentration (5 10⁻⁷ M to 5 10⁻¹¹ M) for 20 min to reach equilibrium conditions between modified electrode and the solution. Then, EIS (Initial potential E = -0.150 V. Highest Freq = 100 kHz, Lowest Freq =100 mHz, amplitude = 10 mV) were used to investigate the charge transfer resistance of the film. EIS measurements were performed in a 0.1 M potassium citrate solution (pH=4). The real and imaginary parts of impedance were computed and a Nyquist plot was drawn. The impedance data were fitted, using EC-Lab software, to a Randles equivalent electrical circuit formed by a combination of a serie resistance R_s (solution and connections) and a charge transfer resistance R_{ct} placed in parallel with a constant phase element CPE. CPE impedance is equal to $1/Q(j\omega)^n$, where Q is the capacitance (F.s⁻¹) and n is between 0 and 1.

1.3. Synthesis of Reagents and Monomers

Diethylphosphonate-containing bisphenols (compounds 1 and 2) were preliminary prepared, according to multi-step syntheses, as represented in Fig. 1 and Fig. 2. Bisphenol 1 procedure was detailed elsewhere [19].

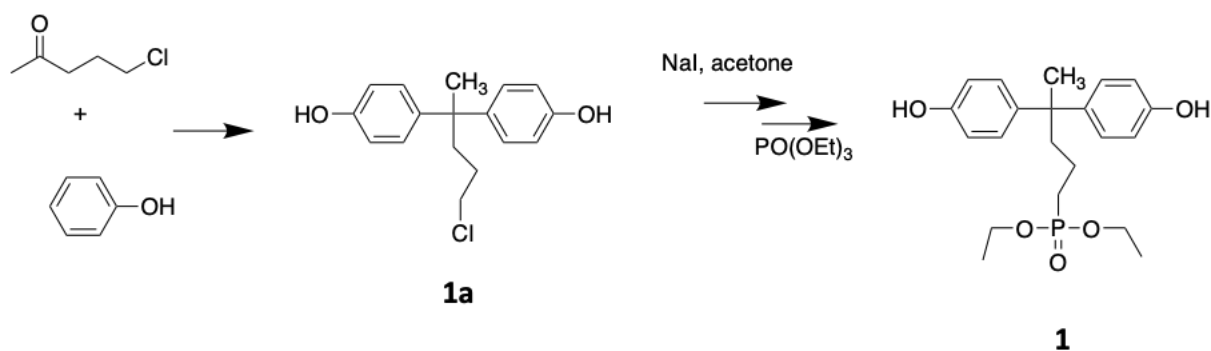


Figure 1. Synthetic pathway for the synthesis of bisphenol 1.

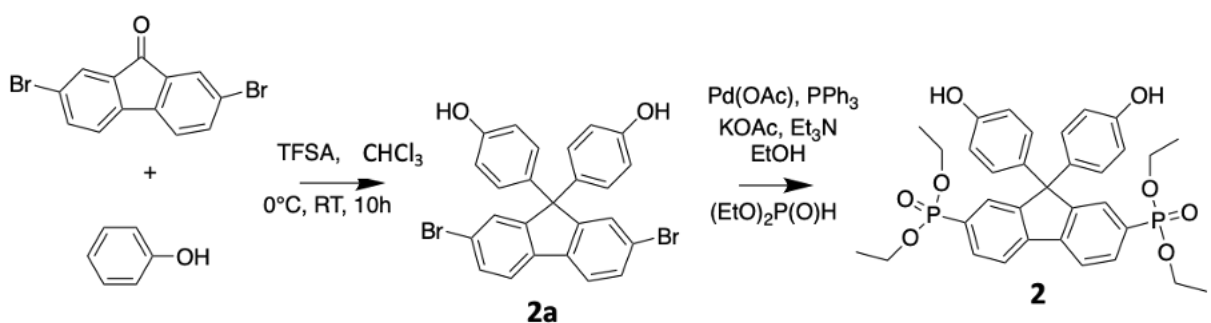


Figure 2. Synthetic pathway for the synthesis of bisphenol 2.

Bisphenol 2 was synthesized according to the following two-step synthesis:

Step 1: In a 500 mL three-necked round bottom flask equipped with a condenser, an addition funnel and a nitrogen inlet, 7.5 g (22.2 mmol) of 2,7-dibromofluorenone and 4.44 g (46.7 mmol) of phenol were suspended in 300 mL of chloroform. The reaction medium was ice-cooled and 4.13 mL (46.7 mmol) of trifluoromethane sulfonic acid (TFSA) were added dropwise. The reaction mixture was stirred at room temperature overnight. The precipitated crude product was isolated by filtration and successively rinsed with chloroform, petroleum ether and water. After drying under vacuum at 80°C, dibromobisphenol **2a** was obtained with 70% yield.

^1H NMR (DMSO- d_6 , 80°C): δ 6.58 (d, 4H), 6.81 (d, 4H), 7.40 (d, 2H), 7.49 (dd, 2H), 7.81 (d, 2H). ^{13}C NMR (DMSO- d_6 , 80°C): 64.62 (C7), 115.89 (C3, C5, C22, C24), 121.48 (C14, C19), 123.01 (C16, C17), 129.05 (C2, C6, C13, C20, C21, C25), 131.06 (C15, C18), 134.88 (C1, C8), 133.08 (C10, C11), 154.55 (C9, C12), 156.95 (C4, C23).

Step 2: 0.25g (1.1 mmol) of palladium acetate, 0.88g (3.3 mmol) of triphenylphosphine (PPh_3) and 1.1 g (11.2 mmol) of potassium acetate were introduced in a 125 mL three-necked

round bottom flask equipped with a condenser, an argon inlet, and a magnetic stirrer. 30 mL of anhydrous ethanol and 3 mL of triethylamine (Et_3N) were added. The reaction mixture was heated at 80°C for 30-40 minutes in order to activate the catalytic system. Once the medium turned red, 6g (11.2 mmol) of **2a** and 2.95g (28 mmol) of diethylphosphite in 24 mL of anhydrous ethanol were added. The reaction mixture was refluxed for 6 hours. After completion of the reaction, the solvent was evaporated. The crude product was rinsed with acetone, deionized water, and dried under vacuum at 80°C . Bisphenol **2** was obtained with 60% yield.

^1H NMR ($\text{DMSO}-d_6$, 80°C): 1.81 (t, 12H), 3.99 (q, 8H), 6.67 (d, 4H), 6.87 (d, 4H), 7.64 (dd, 2H), 7.77 (m, 2H), 8.17 (m, 2H), 9.45 (OH). ^{13}C NMR ($\text{DMSO}-d_6$, 80°C): 16.44 (C33, C36, C39, C42), 62.29 (C34, C37, C40, C43), 64.49 (C7), 115.85 (C4, C6, C22, C24), 121.94, 122.11 (C16, C17), 128.61, 130.46 (C14, C19), 128.89 (C1, C3, C21, 25), 129.08 (C13, C20), 131.26, 131.31 (C15, C18), 134.8 (C2, C8), 142.5 (C10, C11), 153.05 (C9, C12), 156.99 (C5, C23). ^{31}P ($\text{DMSO}-d_6$, 80°C): 17.71 ppm.

1.4 Synthesis of phosphonate ester-containing poly(arylene ether nitrile)s P1-P9

Phosphonate ester-containing poly(aryl ether nitrile)s were synthesized by aromatic nucleophilic substitution, as represented in Figure 3:

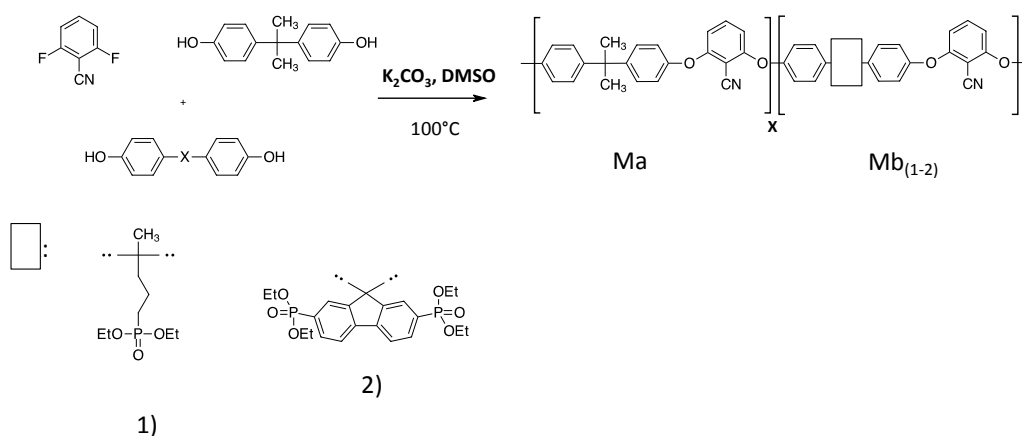


Figure 3. Synthesis of phosphonate ester-containing poly(arylene ether nitrile) by aromatic nucleophilic substitution

In a two-necked round bottom flask equipped with a nitrogen inlet and a mechanical stirrer, 0.436 g (1.91 mmol) of bisphenol A, (1.27 mmol) of diethylphosphonate-containing

bisphenol (**1** or **2**), 0.443 g (3.19 mmol) of 2,6-difluorobenzonitrile, 0.968 g (7.01 mmol) of potassium carbonate and 4.14 mL of DMSO were added. The reaction mixture was heated at 100 °C for two days. After cooling, the medium was poured into water and the white fibrous polymer was collected by filtration, thoroughly rinsed with water and finally dried under vacuum.

1.5 Preparation of Polymer-Modified Gold Electrodes

Pre-treatment of the substrate: Gold substrates (300 nm of gold layer/30 nm of titanium layer/300 nm SiO₂/p-type Si/300 nm SiO₂), provided by the French RENATECH network (LAAS, CNRS Toulouse), were successively rinsed with acetone for 15 minutes, with deionized water, and then dried with nitrogen flow. The gold surface was then immersed alternately for about 3 minutes in a Piranha solution, rinsed with deionized water, and was finally dried under nitrogen flow.

Preparation of polymer-modified electrodes: a solution of the diethylphosphonate-containing poly(arylene ether nitrile)-polymer in chloroform (5 μL, 1w/w%) was dropped on the surface of the gold electrode. Solvent was evaporated under nitrogen flow, at room temperature.

2. Results and Discussion

2.1 Synthesis of phosphonate ester containing poly(arylene ether nitrile)s

2.1.1 Synthesis of diethylphosphonate-containing bisphenols

In the frame of this study, two diethylphosphonate containing bisphenols were synthesized, as represented in Figure 1 and Figure 2. Bisphenol **1** was synthesized in two steps. The chloroalkyl precursor **1a** is synthesized by Friedel-Craft reaction of phenol on 5-chloropentan-2-one. The diethylphosphonate group is then incorporated by an Arbusov reaction. The resulting bisphenol bears only one diethylphosphonate group, which is removed from the monomer backbone vicinity thanks to the presence of the alkyl side-chain spacer. Bisphenol **2** was also synthesized in two steps: a dibromodispirofluorene bisphenol **2a** was obtained by Friedel-Craft reaction of phenol on dibromofluorenone. The phosphonate ester groups were further introduced on this compound, by palladium cross-coupling of the arylbromide with (EtO)₂P(O)H. In this case, the two diethylphosphonate groups are directly linked to the rigid aromatic core of the bisphenol. All physico-chemical characterization (¹H, ¹³C, ³¹P NMR) are reported in supported information (S1-S5).

2.1.2 Synthesis of phosphonate ester containing poly(arylene ether nitrile)s

In the frame of some ongoing work dedicated to the development of new aromatic functional polymers, different diethylphosphonate-containing poly(arylene ether nitrile)s were synthesized by classic step-growth copolymerization of the previously prepared bisphenols with 2,6-difluorobenzonitrile and bisphenol A. This aromatic nucleophilic substitution was performed in a polar aprotic solvent (DMSO) and in the presence of potassium carbonate, in mild conditions (100°C) (Figure 3). The targeted proportions of incorporated Bisphenol A (X %) and of diethylphosphonate ester-containing monomer (Y %) in the final polymer could be easily tuned by adjusting the monomers feed ratio. As bisphenol 1 contains only one diethylphosphonate group and bisphenol 2 contains two diethylphosphonate groups, it is possible to synthesize different polymers having similar proportions of chelating sites, but differently incorporated in the polymer chain.

The number of PO(OEt)₂ groups (expressed in mmol per gram of polymer) can be calculated from equation 1, taking into account the respective proportions of bisphenol A (X%), the diethylphosphonate containing monomer (Y%), the number of diethylphosphonate groups (N) in the functional bisphenol incorporated, and the mean molecular weight of the two repeating units (M_a and M_{b(1-2)}), as represented in Figure 4).

$$PO(OEt)_2 \text{ content (in mmol per g of polymer)} = 1000 \times \frac{Y \times N}{X \times M_a + Y \times M_{b(1-2)}}$$

Equation 1. Calculation of the PO(OEt)₂ content (in mmol per gram of polymer)

As calculated from this equation and as reported in table 1, both P3 and P7 have similar PO(OEt)₂ content (respectively 0.5 and 0.55 mmol/g of polymer), as well as P4 and P8 (1.1 and 1.05 mmol/g of polymer).

Whereas in P1-P6, the diethylphosphonate anchoring sites are incorporated in the macromolecular backbone as side-chains (because of the short alkyl spacer), they are directly linked to the polymer main chain in P7-P9.

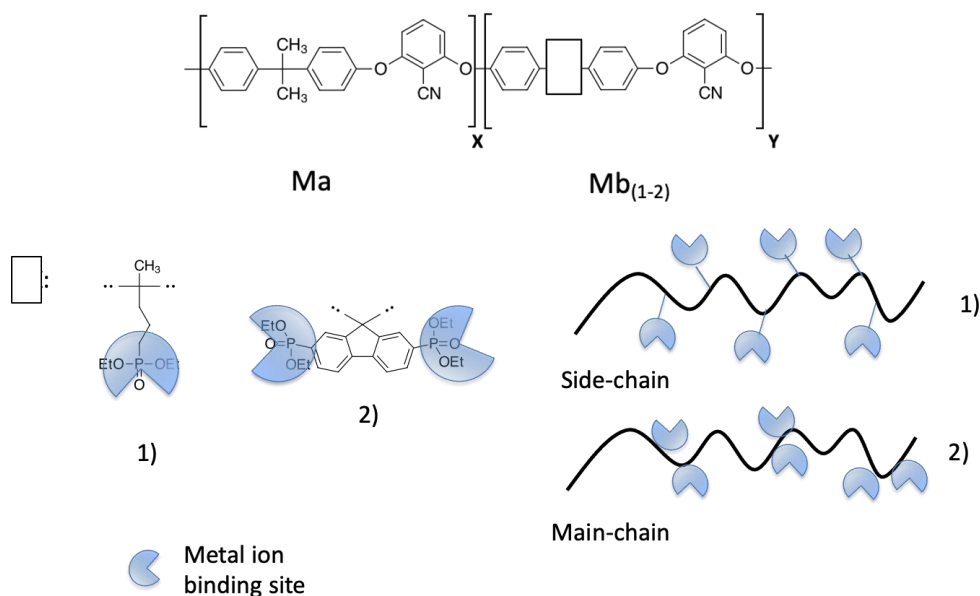


Figure 4. General structure of diethylphosphonate- containing poly(arylene ether nitrile)s M_{b1} and M_{b2} respectively corresponds to the mean molecular weight of the sequences based on bisphenol 1 and bisphenol 2

Table 1 summarizes the structural characteristics of the different synthesized polymers.

Table 1. Structural characteristics of the diethylphosphonate-containing polymers

Reference	Bisphenol	N**	X/Y*	PO(OEt) ₂ content (mmol/g)	T _g (°C)
P1		-	100/0	0	164 ^[16]
P2	Bisphenol 1	1	90/10	0.30	142
P3	Bisphenol 1	1	80/20	0.55	131
P4	Bisphenol 1	1	60/40	1.10	128 ^[16]
P5	Bisphenol 1	1	50/50	1.30	119 ^[16]
P6	Bisphenol 1	1	30/70	1.70	108 ^[16]
P7	Bisphenol 2	2	90/10	0.5	162
P8	Bisphenol 2	2	80/20	1.05	153
P9	Bisphenol 2	2	60/40	1.80	150

* X and Y are respectively the proportions of bisphenol A and diethylphosphonate containing bisphenol

** Number of PO(OEt)₂ groups per diethylphosphonate containing monomer

2.2 Physico-chemical characterization of the polymers

2.2.1 NMR characterization

The chemical structure of the resulting polymers were analyzed by NMR spectroscopy. Whereas P1-P6 spectra were reported elsewhere [19], typical spectra for P7-P9 are reported in supporting information (S6). As an example, the ^1H NMR characterization of both structures containing 40% of phosphonate ester-containing monomer (P4 (60M_a/40M_{b1}) and P9 (60M_a/40 M_{b2})) are reported in Figure 5

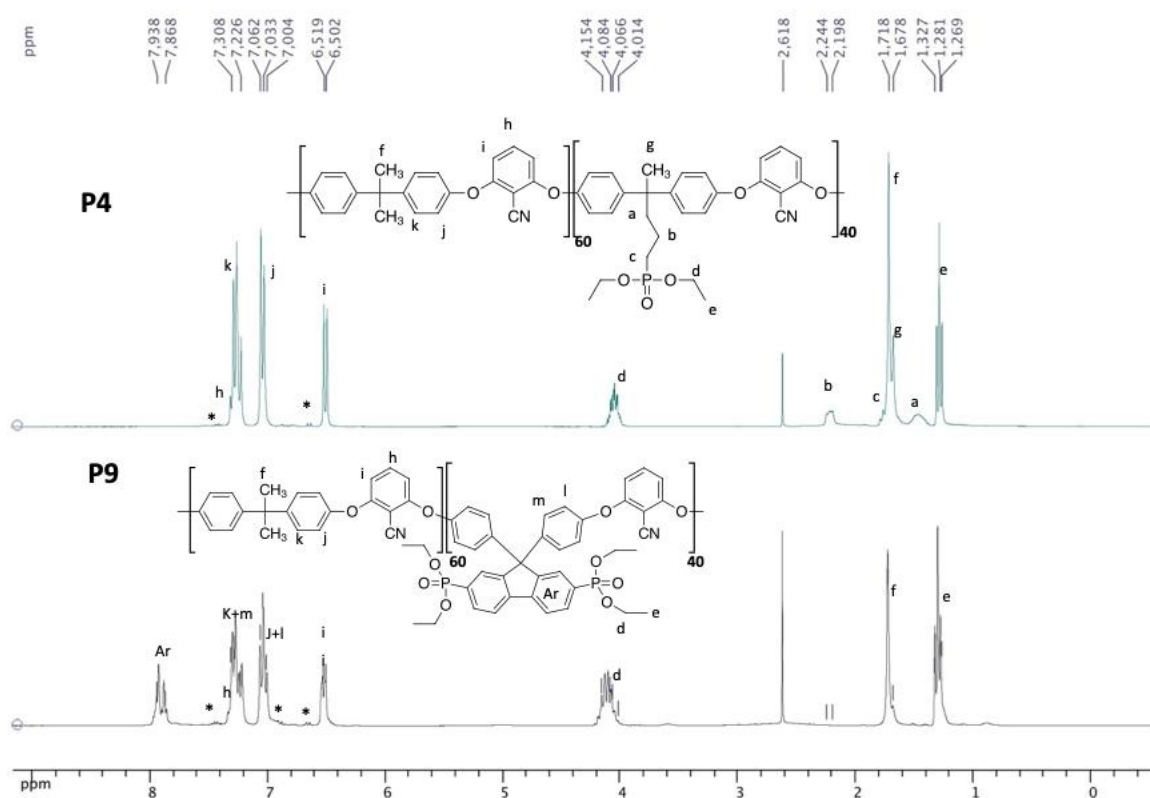


Figure 5. ^1H NMR characterization of diethylphosphonate- containing poly(arylene ether nitrile)s in DMSO- d_6 , Tamb (P4 and P9)

Thorough assignment of the different signals confirms the expected structures. These spectra evidence the effective incorporation of the diethylphosphonate containing monomers involved in the polycondensation, respectively by the presence of protons H_a, H_b, H_c, H_d, H_e, and H_g in P4 and protons H_d, H_e, H_{Ar}, H_m and H_l in P9.

In both cases, by comparing the integration values of H_d (proton belonging to the diethyl phosphonate bisphenol) and H_i (proton belonging to the benzonitrile comonomer), it is possible to calculate the experimental ratio of diethylphosphonate groups-containing

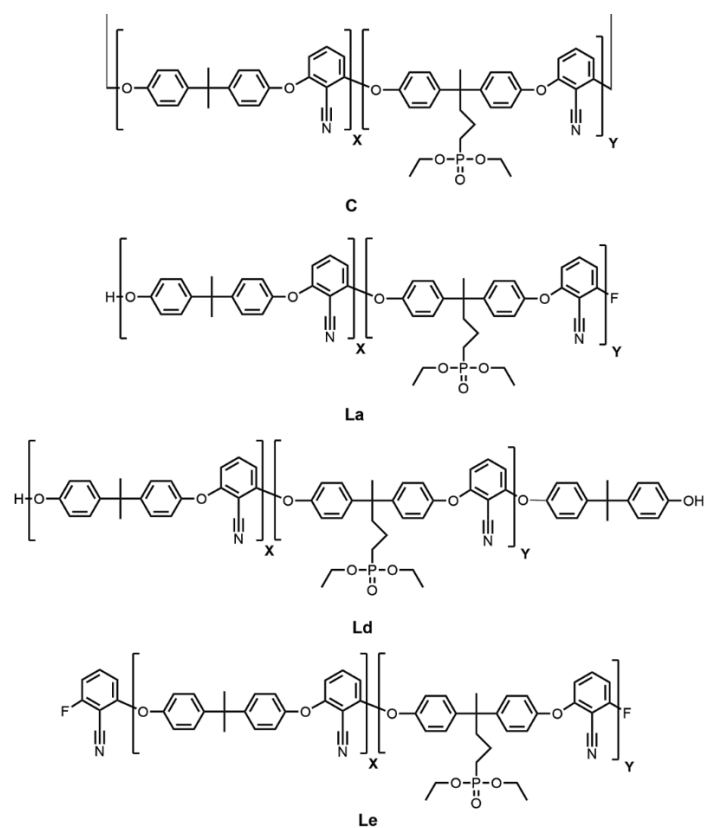
monomer (Y) incorporated during the polycondensation ($Y=(Int_{Hd}/2) /Int_{Hi}$ for P4 and $Y=(Int_{Hd}/4) /Int_{Hi}$ for P9). In both cases, a very good agreement between the experimental and the theoretical proportion of diethyl phosphonate containing monomer were observed ($Y_{exp}=40,9\%$ and $Y_{exp}=41,1\%$ for P4 and P9 respectively).

Additional very low intensity peaks (noted *) are attributed to the presence of eventual polymer chain end groups.

2.2.2 MALDI ToF MS characterization

Poly(arylene ether nitrile)s P4 and P9 were characterized by MALDI ToF MS, in order to study more in depth their chemical composition and clearly identify the polymer chain end-groups. The different structures that could be obtained during their syntheses and their MALDI ToF mass spectra are sum up in Figure 6 (for P4) and Figure 7 (for P9).

Cyclic and linear structures are respectively noted $C_{X,Y}$ and $L(a-e)_{X,Y}$; Y corresponds to the diethylphosphonate containing unit. Letters (a-e) are attributed to different chain end-groups.



Structure	Cyclic : C	Linear : La	Linear : Ld	Linear : Le
MTh	$(327.4 \cdot X) + (491.5 \cdot Y)$	$(327.4 \cdot X) + (491.5 \cdot Y) + 20$	$(327.4 \cdot X) + (491.5 \cdot Y) + 228.29$	$(327.4 \cdot X) + (491.5 \cdot Y) + 193.1$

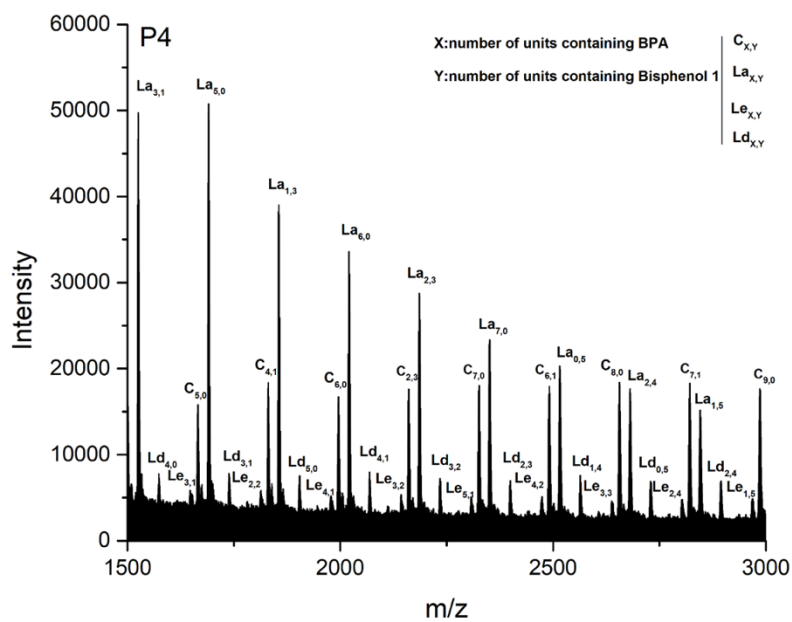
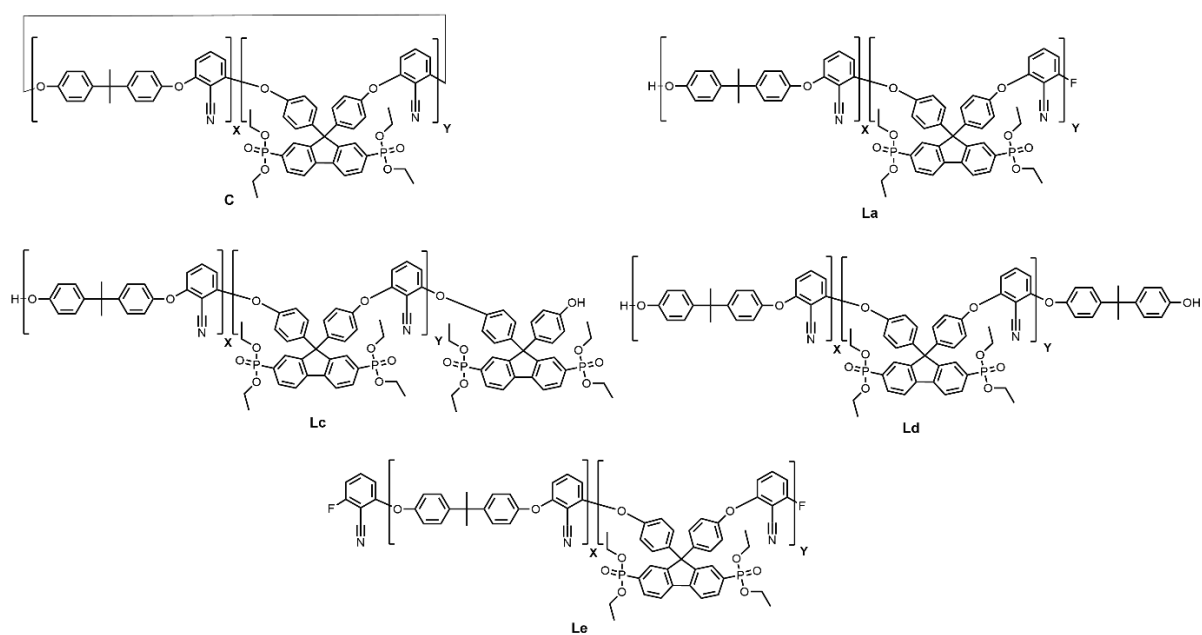


Figure 6. Eventual structures obtained from the polycondensation of bisphenol 1, bisphenol A, and difluorobenzonitrile. Maldi ToF analysis of P4



Structure	Cyclic : C	Linear : La	Linear : Lc	Linear : Ld	Linear : Le
Mth	$(327.4 \cdot X) + (721.7 \cdot Y)$	$(327.4 \cdot X) + (721.7 \cdot Y) + 20$	$(327.4 \cdot X) + (721.7 \cdot Y) + 622.6$	$(327.4 \cdot X) + (721.7 \cdot Y) + 228.3$	$(327.4 \cdot X) + (721.7 \cdot Y) + 193.1$

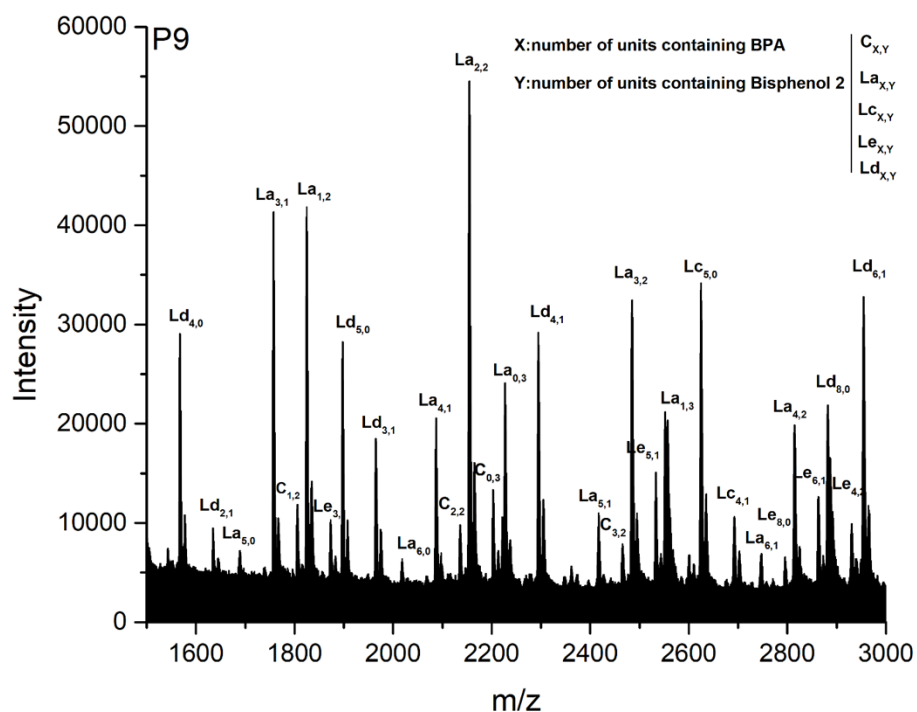


Figure 7. Eventual structures obtained from the polycondensation of bisphenol 2, bisphenol A, and difluorobenzonitrile. Maldi ToF analysis of P9

Careful analyses of the spectra indicate a predominance of linear structures for both P4 and P9, with the presence of less abundant cyclic structures. The results obtained for P4 suggest that most polymer chains are telechelic, having one phenolic end group and one fluorobenzyl ring at the other extremity. Polymer chains terminated at both ends either by phenol groups or halogenated function are also present. However, no polymer chain ended by bisphenol 1 could be evidenced. This observation might induce that bisphenol 1 is slightly more reactive than bisphenol A.

On the other hand, it was possible to identify some P9 chains ended with bisphenol 2 (Lc structures). Therefore, we might conclude that bisphenol 2 and bisphenol A have similar reactivities, and that bisphenol 1 is more reactive than bisphenol 2.

Both for P4 and P9, Maldi ToF spectra attest for the presence of a wide range of repeating units having different compositions, depending on the incorporation of the comonomers involved in the polycondensation. These results are consistent with a random condensation of the diethylphosphonate monomers and of the other comonomers during the polymer synthesis and suggest that diethylphosphonate chelating groups are randomly present in the polymer chains.

2.2.3 Thermal characterization

All polymers are amorphous, as evidenced by DSC analyses. Typical thermograms for P7-P9 are reported in Fig. S7. As mentioned in Table 1, the incorporation of diethylphosphonate groups results in a glass transition temperature decrease. Whereas this effect is rather moderate when the phosphorus-containing groups are directly linked to the macromolecular backbone, the presence of diethylphosphonate groups incorporated in the polymer chain through a short alkyl spacer has a higher impact. Indeed, compared to P1 (0 mmol PO(OEt)₂/g; T_g= 164°C), the glass transition temperature of P8 (1.05 mmol PO(OEt)₂/g) is only slightly decreased (T_g=153°C), whereas the glass transition temperature of P4 (1.1 mmol PO(OEt)₂/g) is much affected (T_g=128°C). This observation is in accordance with the well-known plasticizing effect of short alkyl spacers [21]. The thermo-oxidative stability of the polymers was assessed by thermogravimetry experiments. All polymers are stable up to 250°C. At higher temperatures, the diethylphosphonate group degrades, resulting in the formation of phosphonic acid groups and ethylene, as already reported elsewhere [22-23]. Two phosphonic acid groups might also condense into an anhydride bridge in this temperature range. Typical TGA analyses (P7-P9) are reported in supporting information (Fig. S8).

All polymers were soluble in common organic solvents and could be cast into uniform thin films, from polymer solutions in chloroform.

2.3 Electrochemical characterization

2.3.1 Detection of Pb^{2+} Ion by EIS Measurements

Gold substrates were preliminary coated with the diethylphosphonate-containing polymers (P1-P9), by a drop-coating process. The as-modified electrodes were then equilibrated in different aqueous solutions containing metallic ions. The electrochemical impedance measurements of the polymer-modified gold electrode/electrolyte interface were carried out in the presence of increasing concentrations of lead ions in acetate solution are presented in Figure 8.

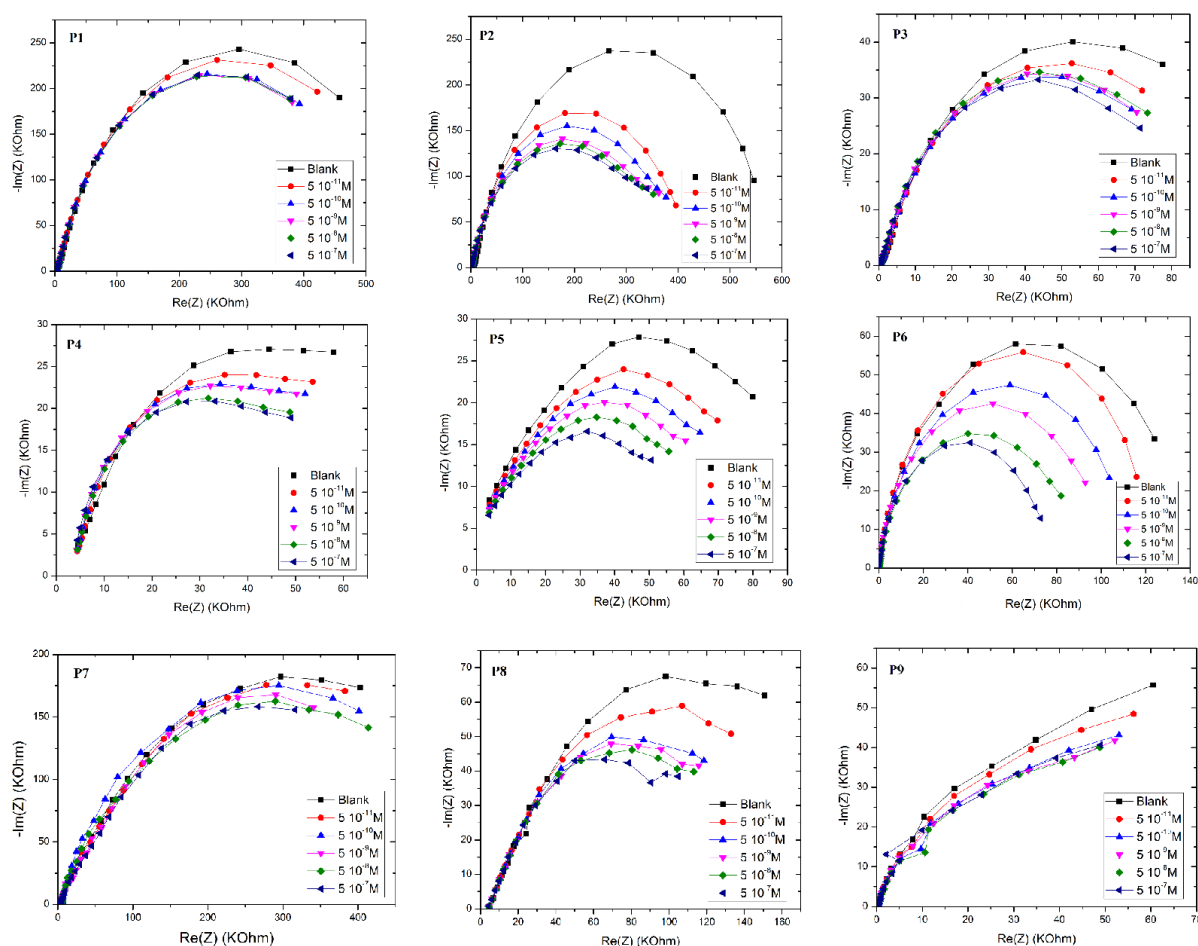
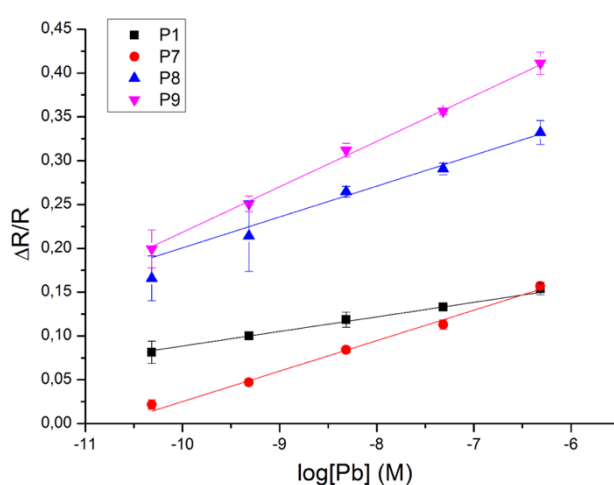
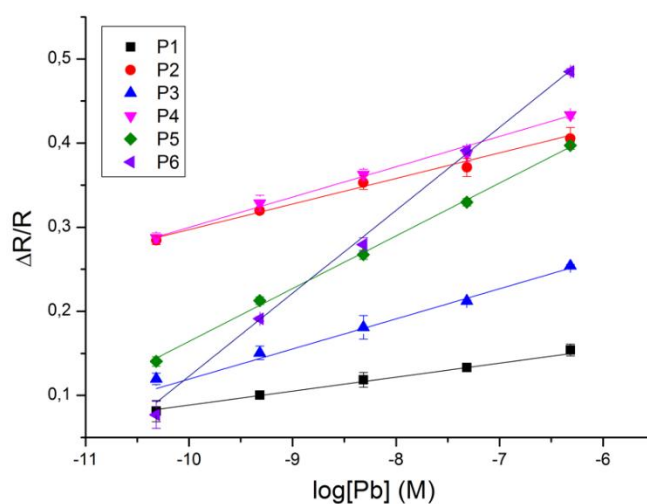


Figure 8. Nyquist plots of the gold electrode/P1-P9/electrolyte obtained in presence of Pb^{2+} ion. Measuring solution: 0.1 M potassium citrate solution at pH 4.0

As shown in Fig. 8, the impedance of the polymer-modified gold electrode/electrolyte interface decreases when the concentration of Pb^{2+} increases. The Nyquist plots were fitted with the standard Randles equivalent circuit using the EC-Lab software. The values of the parameters (R_s , R_{ct} , Q , n) were extracted for every lead concentration and the value of X^2 , showing the quality of fitting (Table S1). The calibration curve of the polymers (P1-P9)-modified gold electrode interface, was obtained by plotting the relative variation of R_{ct} ($\Delta R/R = |R_{ct0} - R_{ct}|/R_{ct}$) versus the co-logarithm concentration of lead ions (Figure 9). The linear range, limits of detection and the sensitivities (defined as the slope of the straight line of $\Delta R/R$ versus log of metal concentration) obtained for the Pb^{2+} ions are reported in Table 2.



(a)



(b)

Figure 9. Relative variation of the polarization resistance of the polymer-modified gold electrode interface as a function of log concentration of Pb^{2+} ion (pM).

Table 2. Comparative study: responses of sensors based on P1-P9 polymers for the Pb²⁺ ion

Sensing polymers	Sensitivity	LOD [M]	Linear range [M]
P1	0.018	5 10 ⁻¹¹	5 10 ⁻¹¹ - 5 10 ⁻⁷
P2	0.029	5 10 ⁻¹¹	5 10 ⁻¹¹ - 5 10 ⁻⁷
P3	0.032	5 10 ⁻¹¹	5 10 ⁻¹¹ - 5 10 ⁻⁷
P4	0.035	5 10 ⁻¹¹	5 10 ⁻¹¹ - 5 10 ⁻⁷
P5	0.065	5 10 ⁻¹¹	5 10 ⁻¹¹ - 5 10 ⁻⁷
P6	0.103	5 10 ⁻¹¹	5 10 ⁻¹¹ - 5 10 ⁻⁷
P7	0.033	5 10 ⁻¹¹	5 10 ⁻¹¹ - 5 10 ⁻⁷
P8	0.041	5 10 ⁻¹¹	5 10 ⁻¹¹ - 5 10 ⁻⁷
P9	0.055	5 10 ⁻¹¹	5 10 ⁻¹¹ - 5 10 ⁻⁷

The relative variation of ($\Delta R/R$) for the polymers modified-electrode P1-P9 is linearly proportional to the co-logarithmic value of Pb²⁺ ion concentration in the range of 50 pM to 0.5 μ M, as shown in Figure 9 (a,b). The dynamic range is 50 pM – 0.5 μ M. The limit of detection was estimated to be 50 pM corresponding to three times the noise of the background divided by the sensitivity. This detection limit is 10² times lower than that obtained by anodic stripping voltammetry on BDD, 5.5 nM [24] and that obtained by potentiometry, 4 nM [25]. The measurements were performed with three different electrodes and the RSD was 2.5%.

As reported in Table 2, the higher sensitivity is obtained with polymer P6. In a series of polymer (P2 to P6 and P7 to P9, the results suggest that one key parameter is related to the amount of diethylphosphonate groups incorporated in the polymer backbone. It clearly appears that the higher the diethylphosphonate content, the better the sensor sensitivity.

However, the presence of a short alkyl spacer which removes the complexing group from the polymer chain seems to be also important to significantly improve the binding efficiency of the polymer, especially for polymers having high content of diethylphosphonate groups.

Indeed, P6 modified gold electrode has by far the best sensitivity, which is almost twice compared to those of the P9-based sensor. These results suggest that both parameters (proportion of binding groups and presence of a short alkyl spacer) might have a synergic effect for the detection of trace levels of lead ions.

2.3.2 Selectivity of polymer (P6) modified gold electrode and its recyclability

Electrochemical impedance measurements were performed in the presence of different metallic ions of the WFD (Ni^{2+} , Hg^{2+} and Cd^{2+}). Each metal was studied separately. The full data of the equivalent circuits are given in Supporting Information (Table S1), for various concentrations of the four WFD metal ions.

The relative variation of the charge transfer resistance ($\Delta R/R$) versus the co-logarithm concentration of the WFD metal ions are presented in Figure 10. Former results obtained for lead ions, described above, are compared to these results in Figure 10. The linear range, the limits of detection and the sensitivities obtained for the different metallic ions are reported in Table 3.

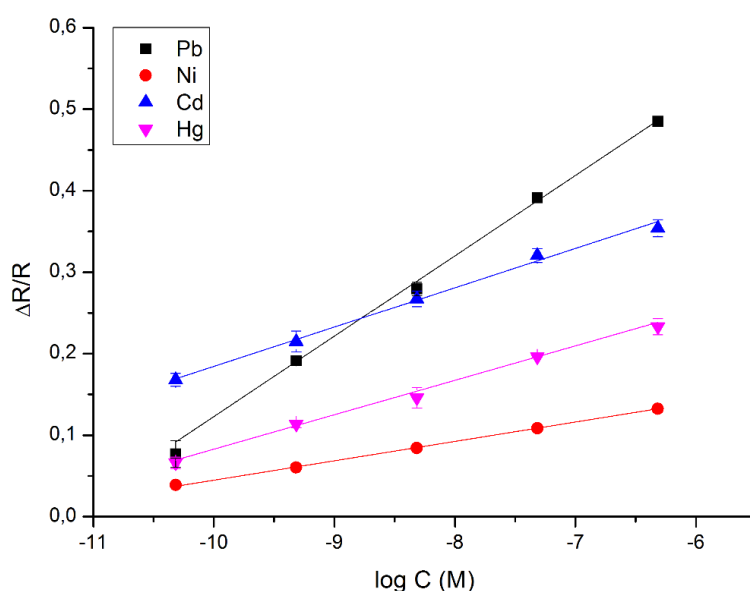


Figure 10. Relative variation of the polarization resistance of the P6 polymer-modified gold electrode interface as a function of heavy metal ion concentration (Pb^{2+} , Ni^{2+} , Hg^{2+} and Cd^{2+} ions).

Table 3. Comparative study: responses of sensors based on polymer P6 for the different ions Pb^{2+} , Ni^{2+} , Cd^{2+} and Hg^{2+}

Ions	Sensitivity	LOD [M]	Linear range [M]
Pb^{2+}	0.103	$5 \cdot 10^{-11}$	$5 \cdot 10^{-11} - 5 \cdot 10^{-7}$
Ni^{2+}	0.022	$5 \cdot 10^{-11}$	$5 \cdot 10^{-11} - 5 \cdot 10^{-7}$
Cd^{2+}	0.047	$5 \cdot 10^{-11}$	$5 \cdot 10^{-11} - 5 \cdot 10^{-7}$
Hg^{2+}	0.041	$5 \cdot 10^{-11}$	$5 \cdot 10^{-11} - 5 \cdot 10^{-7}$

As shown in Table 3, the higher sensitivity of the poly(arylene-ether-nitrile) P6 is obtained for Pb^{2+} . The ratio of the sensitivities for the different metallic ions are the following ones: the

sensitivity for Pb^{2+} is 2.5 times higher than that of Hg^{2+} , 4.7 times higher than that of Ni^{2+} and 2.2 times higher than that of Cd^{2+} . The detection limit obtained with P6 is 50 pM for all the WFD heavy metal ions. When Hg^{2+} , Ni^{2+} , and Cd^{2+} are present at a concentration ten times lower than Pb^{2+} , the contribution of Hg^{2+} and Cd^{2+} will be 4% of the total signal and the contribution of Ni^{2+} will be 2% of the total signal which is in the range of the error. If the concentration of the interfering ions is more than ten times lower, their contribution should be evaluated by another analytical technique.

The original value of the impedance was restored after washing the film with a 0.1M EDTA solution, due to the desorption of the divalent ions. A variation of 5% in the sensitivity was observed after ten adsorption-desorption cycles.

Conclusion

This article describes the elaboration and characterization of diethylphosphonate groups-containing polymers coated electrodes as sensors for the detection of heavy metals traces, by electrochemical impedance spectroscopy.

The influence of the macromolecular structure on the sensing response was studied, for the detection of Pb^{2+} . The sensitivity of detection increases when the number of diethylphosphonate groups increases. Polymer P6, including the higher amount of diethylphosphonate groups removed from the polymer chain by a short alkyl spacer gave the higher sensitivity of detection of lead ion, with a detection limit of 50 pM. The sensitivity for Pb^{2+} is 2.5 times higher than that of Hg^{2+} , 4.7 times higher than that of Ni^{2+} and 2.2 times higher than that of Cd^{2+} . This novel impedimetric sensor is a good candidate for on-line monitoring of Pb^{2+} during the treatment of wastewater generated by industrial activities.

Author Contribution statement: Conceptualization, Regis Mercier; investigation, Catherine Marestin, Taha Chabbah; methodology, Steffen M. Weidner; writing—original draft preparation, Saber Chatti; writing—review and editing, Nicole Jaffrezic-Renault.

Acknowledgements

The authors thank Edouard Chauveau for assistance in organic and polymer synthesis.

We would like to acknowledge the financial support of CAMPUS-FRANCE and the French Embassy in Tunisia (Dr. Pierre Durand de Ramefort) for the SSHN grant, of the POLYAM project, of the High Ministry of Education and Research in Tunisia for doctoral grant. Region Auvergne Rhone Alpes is acknowledged for the Pack Ambition International Project, EMBAI #246413. CNRS is acknowledged for the IRP NARES. The research leading to these results has received funding from the European Union Horizon 2020 (TUNTWIN) research and innovation program under grant agreement n° 952306. The authors acknowledge the financial support of the EU H2020 WIDESPREAD Program entitled Bionanosens grant agreement # 951887.

References

- [1] European Commission, EC, Commission Implementing Decision (EU) 2018/840 of 5 June 2018. *Off. J. Eur. Union* (2018), 141, 9.
- [2] D.E. Bustos, J.A. Toro, M. Briceno, R.E. Rivas, *Use of slow atomization ramp in high resolution continuum source graphite furnace atomic absorption spectrometry for the simultaneous determination of Cd and Ni in slurry powdered chocolate samples*, *Talanta* (2022), 247, 123547.
- [3] N. Manoussi, E. Deliyanni, G. Zachariadis, *Multi-Element Determination of Toxic and Nutrient Elements by ICP-AES after Dispersive Solid-Phase Extraction with Modified Graphene Oxide*, *Appl. Sci.* (2020), 10(23), 8722.
- [4] W. Ni, X.J.; Mao, M.X. Yao, X.R. Guo, Q.L. Sun, X.F. Gao, H.L. Zhang, *Bismuth fire assay preconcentration and empirical coefficient LA-ICP-MS for the determination of ultra-trace Pt and Pd in geochemical samples*, *Scientific reports* (2022), 12(1), 11555.
- [5] R. Morteza, *Pb(II)-Imprinted Polymers for Construction of Lead-Selective Electrochemical Sensors*, *Analytical & Bioanalytical Electrochemistry* (2022), 14(2) 144.
- [6] YY. Chen, YM. Zhou, QZ. Yao, YY. Bu, HC. Wang, WD. Wu, W. Sun, *Preparation of a Low-Phosphorous Terpolymer as a Scale, Corrosion Inhibitor, and Dispersant for Ferric Oxide*, *J. Appl. Polym. Sci.* (2015), 132(6), 41447/1.
- [7] A. Ghorai, S. Banerjee, *Phosphorus-containing aromatic polymers: Synthesis, structure, properties and membrane-based applications*. *Progress in polymer science*, (2023), 138, 101646).
- [8] H. Tokuyama, K. Yanagawa, S. Sakohara, *Temperature swing adsorption of heavy metals on novel phosphate-type adsorbents using thermosensitive gels and/or polymers*, *Sep. Purif. Technol.* (2006), 50, 8.
- [9] T. Chabbah, S. Chatti, F. Zouaoui, I. Jlalía, H. Gaiji, H. Abderrazak, H. Casabianca, R. Mercier, S. Weidner, A. Errachid, C. Marestin, N. Jaffrezic-Renault, *New poly(ether-phosphoramidate)s sulfides based on green resources as sensitive films for the specific impedimetric detection of nickel ions*. *Talanta*, (2022), 247, 123550.
- [10] S. Monge, B. Canniccioni, A. Graillot, J.J. Robin, *Phosphorus-containing polymers A great opportunity for the biomedical field*, *Biomacromolecules*, (2011), 12, 1973.
- [11] V. Deluchat, S. Lacour, B. Serpaud, J.C. Bollinger, *Washing powders and the environment: has TAED any influence on the complexing behaviour of phosphonic acids*, *Water Res.* (2002), 36, 4301.
- [12] G.T. Eom, S.Y. Oh, T.G. Park, *In situ thermal gelation of water-soluble poly(N-isopropylacrylamide-co-vinylphosphonic acid)*, *J. Appl. Polym. Sci.* (1998), 70, 1947.
- [13] B. Nowack, *Environmental chemistry of phosphonates*, *Water Res.* (2003), 37, 2533.
- [14] V. Deluchat, J.C. Bollinger, B. Serpaud, C. Caillet, *Divalent cations speciation with three phosphonate ligands in the pH-range of natural waters*, *Talanta*, (1997), 44, 897.
- [15] C. Vogel, J. Meier-Haack, *Preparation of ion-exchange materials and membranes*, *Desalination*, (2014), 342, 156.
- [16] E. Abouzari-Loft, H. Ghassemi, A. Shockravi, T. Zawodzinski, D. Schiraldi, *Phosphonated poly(arylene ether)s as potential high temperature proton conducting materials*, *Polymer*, (2011), 52, 4709-4717)
- [17] E. Abouzari-Loft, H. Ghassemi, S. Mehdipour-Ataei, A. Shockravi, *Phosphonated polyimides: enhancement of proton conductivity at high temperatures and low humidity*. *Journal of Membrane Science* (2016), 516, 74.

- [18] W. Archer, N. Iftexhar, A. Fiorito, S. Winn, M. Schulz, *Synthesis of Phosphonated Polymer Resins for the Extraction of Rare-Earth Elements*, ACS Appl Polym Mater, (2022), 4, 2506.
- [19] C. Marestin, R. Mercier, S. Chatti, *Synthesis of poly(aryl ether)s bearing phosphonated side-chains from phosphonate ester-containing bisphenols*, Polymer, (2021), 222, 123647.
- [20] I. Koehne, A. Lik, M. Gerstel, C. Bruhn, J. P. Reithmaier, M. Benyoucef, R. Pietschnig, *Functionalised phosphonate ester supported lanthanide (Ln = La, Nd, Dy, Er) complexes* Dalton Trans., (2020), 49, 16683.
- [21] "Principle of Polymerization", second edition, G. Odian, Wiley 1981.
- [22] I. Cabasso; J. Jagur-Grodzinski, D. Vofsi, *Synthesis and Characterization of polymers with pendent phosphonate groups*, Journal of polymer Science, (1974), 18, 1969.
- [23] Kotov, S.V., Pedersen, S.D., Qiu, W., Qiu, Z.-M. and Burton, D.J., (1997) Preparation of perfluorocarbon polymers containing phosphonic acid groups. *J. Fluorine Chem.*, **82**(1), 13.
- [24] A. Sbartai, P. Namour, F. Barbier, J. Krejci, R. Kunceriva, T. Krejci, V. Nedela, J. Sobota, N. Jaffrezic-Renault, *Electrochemical performances of diamond like carbon films for Pb (II) detection in tap water using differential pulse anodic stripping voltammetry technique*. Sens. Lett. (2013), 11, 1524.
- [25] M. R. Yaftian, M. Parinejad, D. Matt, *A lead-selective membrane electrode based upon a phosphorylated hexahomotrioxacalix[3]arene*. J. Chin. Chem. Soc. (2007), 54(6), 1535.

Impedimetric sensors based on diethylphosphonate-containing poly(arylene ether nitrile)s films for the detection of lead ions

Taha Chabbah⁽¹⁾, Saber Chatti⁽¹⁾, Nicole Jaffrezic-Renault⁽²⁾, Steffen Weidner⁽³⁾
Catherine Marestin⁽⁴⁾, Regis Mercier⁽⁴⁾

- ⁽¹⁾ National Institute of Research and Physico-chemical Analysis (INRAP), Biotechnopole of Sidi Thabet, 2020 Ariana, Tunisia
- ⁽²⁾ University of Lyon, Institute of Analytical Sciences (ISA), UMR 5280, 5 Rue de la Doua, 69100 Villeurbanne, France
- ⁽³⁾ Bundesanstalt für Materialforschung und prüfung (BAM) Fachbereich 6.3 “Strukturanalytik” Richard-Willstätter-Strasse 11, 12489 Berlin Germany
- ⁽⁴⁾ University of Lyon, INSA-Lyon, CNRS, IMP UMR 5223, F-69 621 Villeurbanne Cedex, France

Supporting information

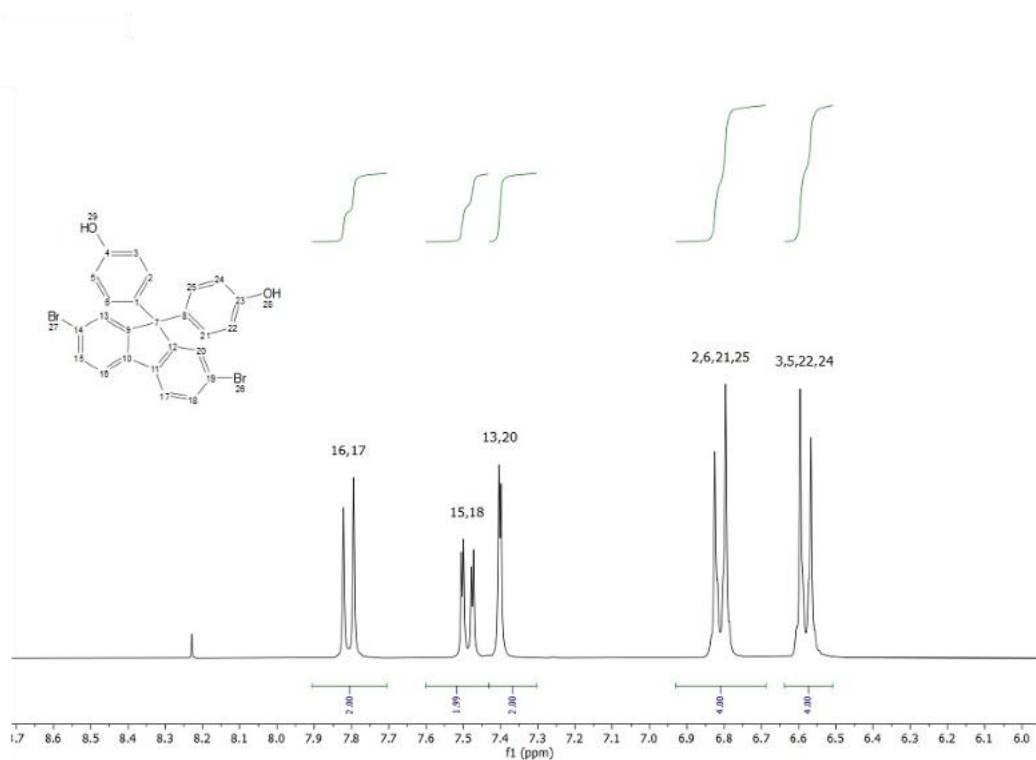


Figure S1. ¹H NMR (DMSO-*d*₆, 80°C) of **2a**

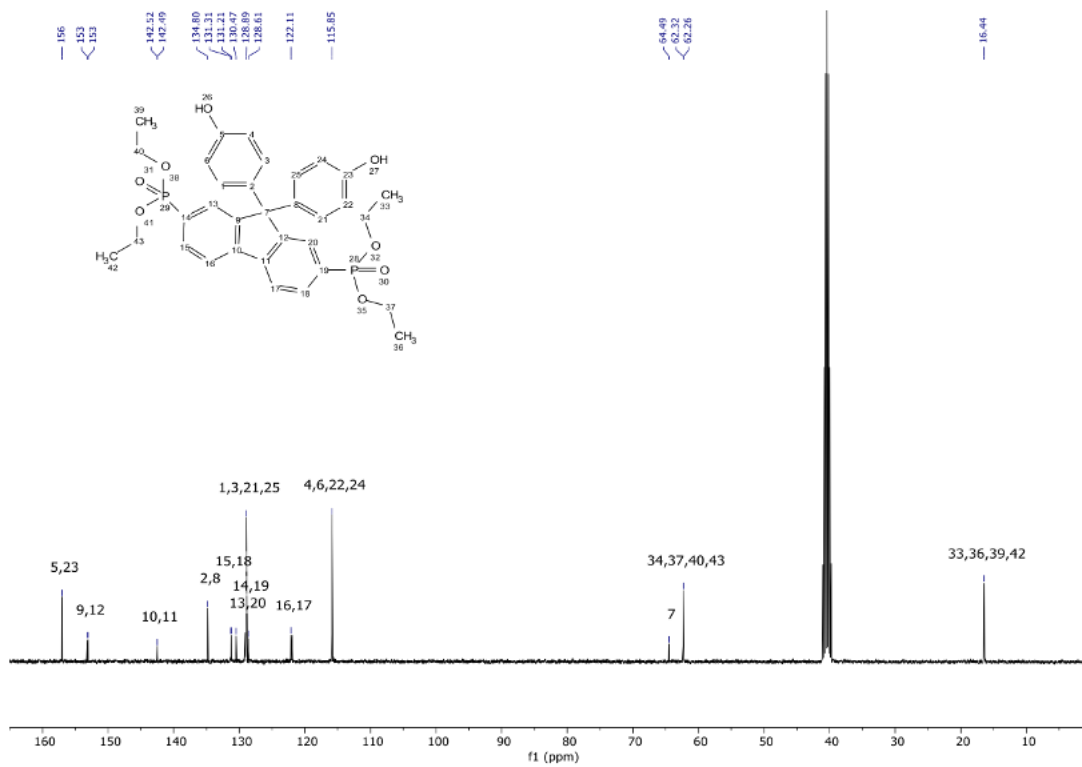


Figure S4. ^{13}C NMR (DMSO- d_6 , 80°C) of 2

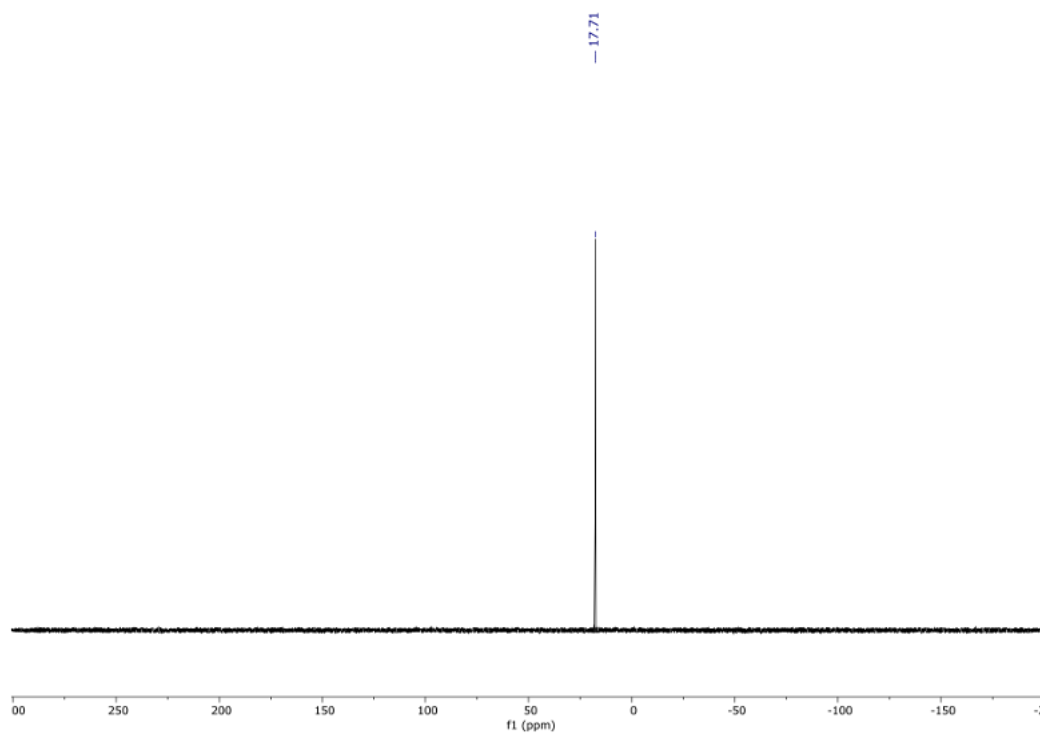


Figure S5. ^{31}P NMR (DMSO- d_6 , 80°C) of 2

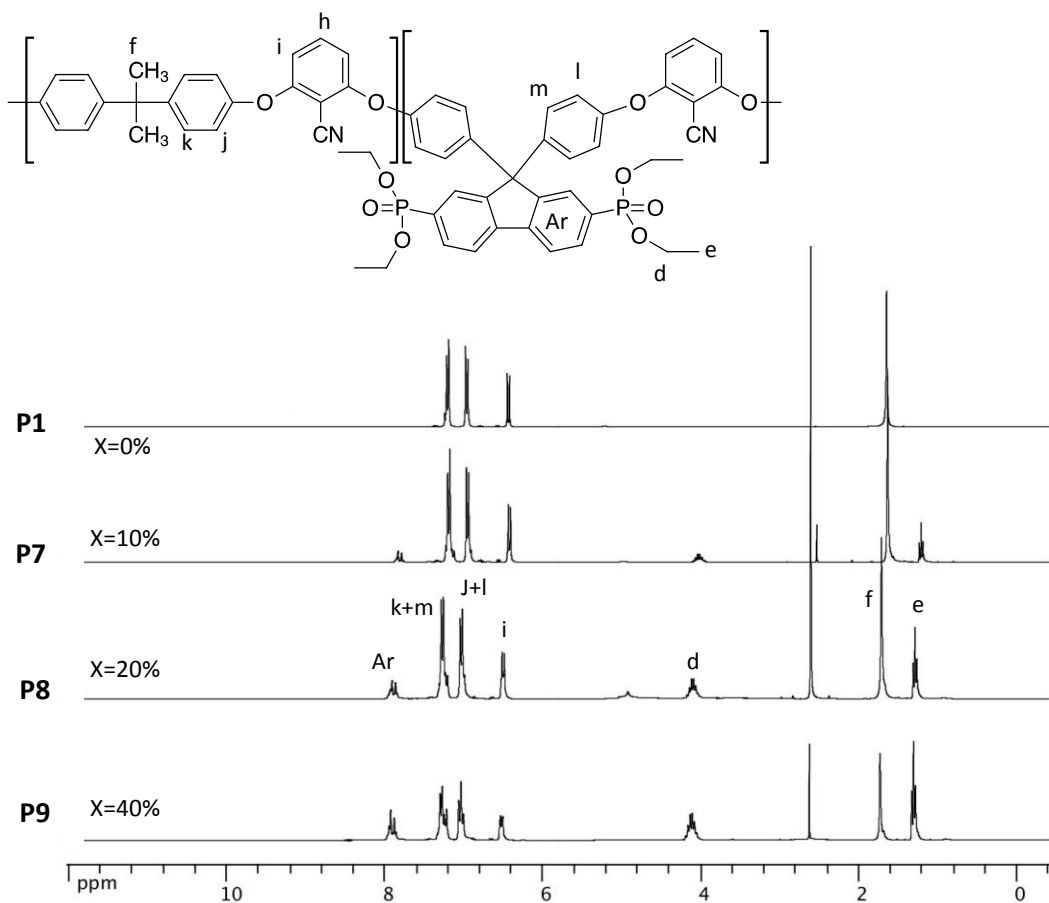


Figure S6. ^1H NMR (DMSO- d_6) of P1, P7, P8, P9. (DMSO- d_6 , 80°C)

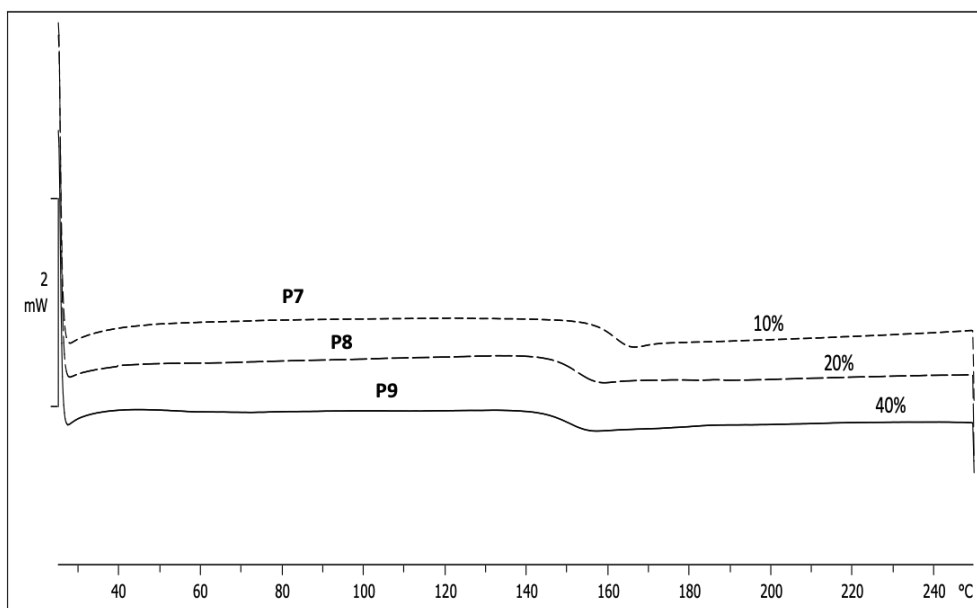


Figure S7. Differential scanning calorimetry analyses of P7-P9

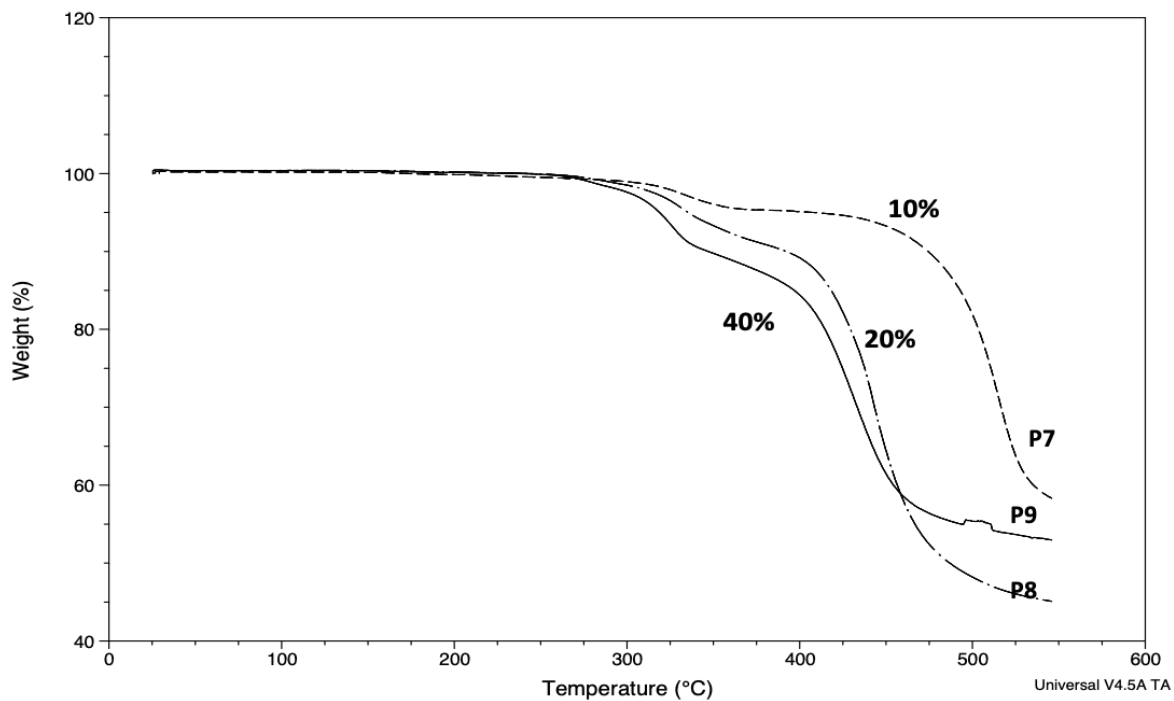


Figure S8. Thermogravimetric analyses of P7-P9 , **under air, at 10°C/min**

Table S1. Parameters of the electrical circuit equivalent to the gold electrode based on the polymer P6 film for different concentration of the cations $X = \text{Pb}^{2+}$, Ni^{2+} , Cd^{2+} and Hg^{2+} .

X	[X] mol /L	0	$5 \cdot 10^{-11}$	$5 \cdot 10^{-10}$	$5 \cdot 10^{-9}$	$5 \cdot 10^{-8}$	$5 \cdot 10^{-7}$
Pb²⁺	$R_s(\Omega)$	171	283	173	168	174	179
	$R_{ct}(\Omega)$	138989	131636	112129	99256	84462	72262
	$Q(\text{F}\cdot\text{s}^{n-1})$	$3.24 \cdot 10^{-6}$	$2.85 \cdot 10^{-6}$	$3.24 \cdot 10^{-6}$	$3.66 \cdot 10^{-6}$	$3.25 \cdot 10^{-6}$	$3.04 \cdot 10^{-6}$
	n	0.88	0.88	0.89	0.90	0.88	0.89
	X^2	0.022	0.011	0.020	0.022	0.036	0.023
Ni²⁺	$R_s(\Omega)$	359	366	381	377	384	421
	$R_{ct}(\Omega)$	16096	15515	15148	14714	14368	13944
	$Q(\text{F}\cdot\text{s}^{n-1})$	$0.97 \cdot 10^{-9}$	$0.97 \cdot 10^{-9}$	$1.04 \cdot 10^{-9}$	$1.08 \cdot 10^{-9}$	$1.19 \cdot 10^{-9}$	$1.27 \cdot 10^{-9}$
	n	0.79	0.79	0.79	0.79	0.78	0.78
	X^2	0.098	0.095	0.091	0.090	0.092	0.082
Cd²⁺	$R_s(\Omega)$	509	513	491	539	508	482
	$R_{ct}(\Omega)$	10412	8715	8271	7775	7199	6802
	$Q(\text{F}\cdot\text{s}^{n-1})$	$1.11 \cdot 10^{-9}$	$1.13 \cdot 10^{-9}$	$1.26 \cdot 10^{-9}$	$1.37 \cdot 10^{-9}$	$1.34 \cdot 10^{-9}$	$1.33 \cdot 10^{-9}$
	n	0.78	0.78	0.78	0.77	0.78	0.78
	X^2	0.075	0.073	0.071	0.083	0.090	0.087
Hg²⁺	$R_s(\Omega)$	126	125	133	102	137	117
	$R_{ct}(\Omega)$	65272	60908	57431	54556	52421	49255
	$Q(\text{F}\cdot\text{s}^{n-1})$	$2.10 \cdot 10^{-6}$	$2.33 \cdot 10^{-6}$	$2.45 \cdot 10^{-6}$	$2.60 \cdot 10^{-6}$	$1.86 \cdot 10^{-6}$	$1.71 \cdot 10^{-6}$
	n	0.87	0.86	0.86	0.86	0.87	0.86
	X^2	0.031	0.023	0.047	0.063	0.077	0.082